Time-bin-encoding-based remote states generation of nitrogen-vacancy centers through noisy channels*

Su Shi-Lei(苏石磊)[a], Chen Li(陈 丽)[b], Guo Qi(郭 奇)[a],
Wang Hong-Fu(王洪福)[c], Zhu Ai-Dong(朱爱东)[c], and Zhang Shou(张 寿)[a,c]†

[a] *Department of Physics, Harbin Institute of Technology, Harbin* 150001, *China*
[b] *Department of Physics, School of Science, Changchun University, Changchun* 130022, *China*
[c] *Department of Physics, College of Science, Yanbian University, Yanji* 133002, *China*

(Received 24 June 2014; revised manuscript received 9 October 2014; published online 10 December 2014)

We design proposals to generate a remote Greenberger–Horne–Zeilinger (GHZ) state and a W state of nitrogen-vacancy (NV) centers coupled to microtoroidal resonators (MTRs) through noisy channels by utilizing time-bin encoding processes and fast-optical-switch-based polarization rotation operations. The polarization and phase noise induced by noisy channels generally affect the time of state generation but not its success probability and fidelity. Besides, the above proposals can be generalized to n-qubit between two or among n remote nodes with success probability unity under ideal conditions. Furthermore, the proposals are robust for regular noise-changeable channels for the n-node case. This method is also useful in other remote quantum information processing tasks through noisy channels.

Keywords: Greenberger–Horne–Zeilinger state, W state, nitrogen-vacancy centers, noisy channel, time-bin encoding

PACS: 03.67.Pp, 03.67.Mn, 42.50.Dv **DOI:** 10.1088/1674-1056/24/2/020305

1. Introduction

Quantum entanglement lies at the heart of quantum information science and technology and is thought to be the key resource to realize quantum computation and quantum information processing (QIP) tasks,[1–4] such as quantum cryptography,[1] quantum teleportation,[3] quantum secure direct communication,[5] quantum cloning machine,[6] and so on. For the case of a tripartite system, it is well known that there are two kinds of entanglement, one is the Greenberger–Horne–Zeilinger (GHZ) state,

$$|GHZ\rangle = (|000\rangle + |111\rangle)/\sqrt{2}, \tag{1}$$

the other is the W state,

$$|W\rangle = (|001\rangle + |010\rangle + |100\rangle)/\sqrt{3}. \tag{2}$$

The GHZ state is non-equivalent to W state owing to the fact that they cannot be converted to each other by local operations and classical communication. Great efforts have been taken to research both the GHZ and W states since these two states have been shown to have valuable applications in quantum information science.[7–12] Lots of theoretical and experiment schemes have been proposed and reported to generate these two states.[13–23]

Generating remote entanglement is critical for constructing a quantum communication network and realizing long-range quantum information processing.[24,25] Many meaningful schemes have been proposed to generate remote entangled states[26] or implement quantum computation[27,28] in distant participants. For the theoretical long distance quantum information processing case, the noise is not seriously considered in general. But it is one of the most important problems in experiments and practical applications since the quantum system would inevitably couple with its environment. This interaction will decrease the reliability of the quantum channel or even cause the quantum states to be changed.[29,30] Some schemes, such as entanglement purification,[31–34] error correction,[35–38] and quantum repeaters[39,40] have been proposed to solve this problem. In contrast to the above schemes, Song *et al*. proposed a robust scheme[41] to generate a remote atomic W state in a polarization noisy channel through an interesting method, i.e. time-bin encoding, which was first proposed by Brendel *et al*.[42] and used widely in QIP tasks.[43–53] The polarization noise in their scheme had no influence on the fidelity of generating the intended state but it would reduce the total success probability to $(1/2)^{n-1}$ for n nodes. In addition, Huang *et al*. proposed a fault tolerant quantum secure direct communication against collective noise.[54] Wu *et al*. also proposed three quantum dialogue protocols under the condition of collection noise.[55]

Recently, a novel solid-state QIP system, the NV center in diamond, has been examined intensively[56] because it

*Project supported by the National Natural Science Foundation of China (Grant Nos. 11264042, 61465013, 11465020, and 11165015), the Program for Chun Miao Excellent Talents of Jilin Provincial Department of Education (Grant No. 201316), and the Talent Program of Yanbian University of China (Grant No. 950010001).

†Corresponding author. E-mail: szhang@ybu.edu.cn

© 2015 Chinese Physical Society and IOP Publishing Ltd

has optical controllability and good long-lived spin triplets, even at room temperature.[57] To generate entanglement, the NV center is always designed to couple to one of the following resonators, i.e. nanomechanical resonators (NAMRs)[58] and MTRs[59,60] with a quantized whispering-gallery mode (WGM),[19,61] or embed in cavities.[62,63] During these apparatus, the NV center coupled to MTRs with a quantized WGM is highly competitive because the required Q factor of the MTR can be surely degraded when it couples to a fiber, which allows the photons to be inputted and outputted on demand through fibers. This feature enables researchers to deterministically generate entanglement of different NV centers in a scalable fashion. Experimentally, by using microspheres,[64,65] diamond-GaP microdisks,[66] and SiN photonic crystals,[67] a strong coupling has been demonstrated between the NV center and the WGM. Besides, MTRs or MTRs-like equipment have been paid more attention since single-photon input–output process with the MTR coupling to atom has been reported.[59] Moreover, the quantum non-demolition measurement for the electronic spin state of diamond NV centers has been proposed[68] and experimentally demonstrated.[69] These works have shown that an NV center coupled to MTR is a suitable platform for QIP tasks.

Inspired by the above researches, we propose to generate remote an n-qubit GHZ state and a W state of NV centers coupled to MTRs through noisy channels by using time-bin encoding processes and fast optical switches. The polarization and phase noise induced by noisy channels generally affect the time of state generation but not its success probability and fidelity. The structure of this paper is arranged as follows. In Section 2, we briefly introduce the rationale of the basic model. In Section 3, we describe the process to generate the four-qubit GHZ state and W state through a noisy channel in two nodes. In Section 4, the method to generalize the proposals to n-qubit is given through regular noise-changeable channels among n nodes. A discussion and conclusion are given in Section 5.

2. Basic model

The NV centers considered here are negatively charged with six electrons from the nitrogen and three carbons surrounding the vacancy. The ground state are electronic spin triplet states $|0\rangle$ ($m_s = 0$), $|+1\rangle$ ($m_s = 1$), and $|-1\rangle$ ($m_s = -1$). The six excited states are recorded as $|A_1\rangle$, $|A_2\rangle$, $|E_x\rangle$, $|E_y\rangle$, $|E_1\rangle$, and $|E_2\rangle$.[61,70] Ground states $|0\rangle$ and $|\pm 1\rangle$ are split with a gap of 2.87 GHz as a result of spin–spin interactions. The excited states are eigenvectors of the full Hamiltonian, which consists of a spin–spin interaction and a spin–orbit interaction without any perturbation. The pair (A_1, A_2) is split from the others at about 5.5 GHz owing to the spin–orbit interaction. The gap between states $|A\rangle_1$ and $|A\rangle_2$ would be increased to 3.3 GHz through the spin–spin interaction. Consequently, state $|A\rangle_2$ would decay to sublevels $|-1\rangle$ and $|+1\rangle$ with emitting left (L) and right (R) polarization photons because state $|A\rangle_2$ is robust with the stable symmetric properties in the limit of low strain, which has been demonstrated in Ref. [70]. With the aim of detecting ground state information conveniently and obtaining appropriate state transformation process, an external magnetic field B_0 along the NV center symmetry axis should be introduced to the split states $|-1\rangle$ and $|+1\rangle$. The effective energy levels of the NV centers used throughout our proposal are $|A\rangle_2$, $|+1\rangle$, and $|-\rangle$, respectively. A sketch drawing is shown in Fig. 1. Considering a process where a single-photon pulse with frequency $\omega_{\rm in}$ inputs in an MTR cavity with the cavity mode frequency $\omega_{\rm c}$, and interacts with the NV center through input–output process. Because the qubits are encoded in states $|-1\rangle$ and $|+1\rangle$, the weak excitation condition, i.e. $\langle\sigma_z\rangle = -1$, should be satisfied throughout this paper. By combining the Heisenberge motion equations of the NV center lowing operators (σ_-) and cavity field operator (a), and the input–output relationship $a_{\rm out}(t) = a_{\rm in}(t) + \sqrt{\kappa}a(t)$, we can achieve the reflection coefficients[61,71–73]

$$r(\omega_{\rm in}) = \frac{[{\rm i}(\omega_{\rm c}-\omega_{\rm in})-\kappa/2][{\rm i}(\omega_0-\omega_{\rm in})+\gamma/2]+g^2}{[{\rm i}(\omega_{\rm c}-\omega_{\rm in})+\kappa/2][{\rm i}(\omega_0-\omega_{\rm in})+\gamma/2]+g^2}, \quad (g\neq 0), \tag{3a}$$

$$r_0(\omega_{\rm in}) = \frac{{\rm i}(\omega_{\rm c}-\omega_{\rm in})-\kappa/2}{{\rm i}(\omega_{\rm c}-\omega_{\rm in})+\kappa/2}, \quad (g=0), \tag{3b}$$

where ω_0, κ, γ, and g denote the transition frequency between states $|A_2\rangle$ and $|-1\rangle$, cavity damping rate, NV center dipolar decay rate, and the coupling coefficient between cavity and NV center, respectively. Under the condition $\omega_{\rm c} = \omega_0 = \omega_{\rm in}$, the reflection coefficients would be simplified to

$$r(\omega_{\rm in}) = \frac{4g^2-\kappa\gamma}{4g^2+\kappa\gamma}, \quad (g\neq 0), \tag{4a}$$

$$r_0(\omega_{\rm in}) = -1, \quad (g=0). \tag{4b}$$

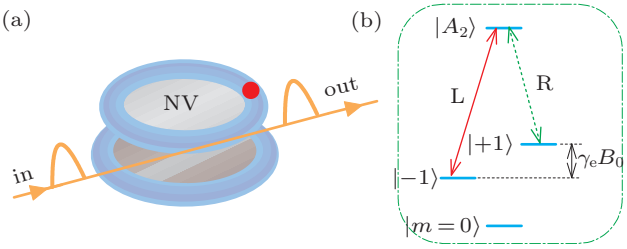


Fig. 1. (color online) A schematic diagram of the single photon input–output process. (a) The NV center fixing on the exterior surface of MTR and interacting with the single photon through input–output process. (b) The effective configuration of the NV center. The transformation from state $|-1\rangle$ to $|A_2\rangle$ is driven resonantly by the input L-polarized single photon. The transformation from state $|+1\rangle$ to $|A_2\rangle$ will not happen in the present scheme due to large detuning caused by the level splitting. B_0 is an external magnetic field along the NV center symmetry axis to split $|\pm 1\rangle$ state. γ_e is the electron gyromagnetic ratio.

After choosing coupling strength $g \geqslant 5\sqrt{\kappa\gamma}$, the reflection coefficient in Eq. (4a) is reduced to $r(\omega_{\rm in}) = 1$. Based on the above analysis, the controlled phase flip gate could be realized between the input pulse and NV center energy levels, which could be expressed as

$$\begin{aligned} &|R\rangle|+1\rangle = +|R\rangle|+1\rangle, \quad |R\rangle|-1\rangle = +|R\rangle|-1\rangle, \\ &|L\rangle|+1\rangle = +|L\rangle|+1\rangle, \quad |L\rangle|-1\rangle = -|L\rangle|-1\rangle, \end{aligned} \tag{5}$$

after applying a phase shifter with π phase on the output pulse.

3. Generating remote four-qubit GHZ and W states between two nodes through a noisy channel

3.1. GHZ state

We now describe the process of GHZ state generation through a noisy channel via time-bin encoding. The sketch of the whole process is shown in Fig. 2. Assuming that the input photon is prepared in the state $(|R\rangle + |L\rangle)/\sqrt{2}$ and the four NV centers are prepared in state $(|+1\rangle + |-1\rangle)/\sqrt{2}$. For convenience, we introduce a usual encoding method, $|+\rangle \equiv (|+1\rangle + |-1\rangle)/\sqrt{2}$, $|-\rangle \equiv (|+1\rangle - |-1\rangle)/\sqrt{2}$. The initial state of the whole system could be written as

$$|\Psi\rangle_1 = \frac{1}{\sqrt{2}}(|R\rangle + |L\rangle)|+\rangle_1|+\rangle_2|+\rangle_3|+\rangle_4. \tag{6}$$

After photon passing through $\rm PBS_1$, $\rm NV_1$, $\rm NV_2$, and $\rm PBS_2$, the state of the whole system is transformed to

$$|\Psi\rangle_2 = \frac{1}{\sqrt{2}}(|R\rangle_{L_0}|+\rangle_1|+\rangle_2 + |L\rangle_{L_1}|-\rangle_1|-\rangle_2)|+\rangle_3|+\rangle_4, \tag{7}$$

where the subscripts L_0 and L_1 correspond to the possible paths L_0 and L_1, respectively. A similar representing method will be used in the following discussion. After the optical switches $\rm S_1$ and $\rm S_2$, the whole system state evolves to

$$|\Psi\rangle_3 = \frac{1}{\sqrt{2}}(|R\rangle_{L_0}|+\rangle_1|+\rangle_2 + |R\rangle_{L_1}|-\rangle_1|-\rangle_2)|+\rangle_3|+\rangle_4. \tag{8}$$

It is important that the optical switches $\rm S_1$ and $\rm S_2$, transmitted when photon in path L_0 passing through, are adjusted to reflect just before the photon in path L_1 passes through. The corresponding sketch of the time control sequences is shown in Fig. 3. Equation (8) implies that the polarization state of the photon is in $|R\rangle$ state before passing through the noisy channel. This merit enables the photon pulse to see the same noise in the noisy channel, which could be expressed as

$$|R\rangle \xrightarrow{\text{noisy channel}} \mathrm{e}^{\mathrm{i}\varphi}\mu|R\rangle + \mathrm{e}^{\mathrm{i}\omega}\nu|L\rangle, \tag{9}$$

in which $\mathrm{e}^{\mathrm{i}\varphi}$ and $\mathrm{e}^{\mathrm{i}\omega}$ are phase noise, μ and ν are polarization noise parameters and satisfy the relation $|\mu|^2 + |\nu|^2 = 1$. Then, the evolution of the whole system after the photon pulse passes through the noisy channel could be written as

$$\begin{aligned} &|\Psi\rangle_3 \xrightarrow{\text{noisy channel}} \\ &\frac{1}{\sqrt{2}}[(\mathrm{e}^{\mathrm{i}\varphi}\mu|R\rangle + \mathrm{e}^{\mathrm{i}\omega}\nu|L\rangle)_{L_0,L}|+\rangle_1|+\rangle_2 \\ &+(\mathrm{e}^{\mathrm{i}\varphi}\mu|R\rangle + \mathrm{e}^{\mathrm{i}\omega}\nu|L\rangle)_{L_1,L}|-\rangle_1|-\rangle_2]|+\rangle_3|+\rangle_4. \end{aligned} \tag{10}$$

After the photon passes through optical switches $\rm S_3$ and $\rm S_4$, the whole system state is changed to

$$\begin{aligned} |\Psi\rangle_4 = \frac{1}{\sqrt{2}}&[(\mathrm{e}^{\mathrm{i}\varphi}\mu|L\rangle + \mathrm{e}^{\mathrm{i}\omega}\nu|R\rangle)_{L_0,L}|+\rangle_1|+\rangle_2 \\ &+(\mathrm{e}^{\mathrm{i}\varphi}\mu|R\rangle + \mathrm{e}^{\mathrm{i}\omega}\nu|L\rangle)_{L_1,L}|-\rangle_1|-\rangle_2]|+\rangle_3|+\rangle_4. \end{aligned} \tag{11}$$

It should be noted that the optical switches $\rm S_3$ and $\rm S_4$, which are always transmitting when the earlier photon pulse (L_0, L) passes through, are adjusted to reflect just before the later photon pulse (L_1, L) comes. The control sequences of switches $\rm S_5$ and $\rm S_6$, $\rm S_7$ and $\rm S_8$ are the same as $\rm S_3$ and $\rm S_4$. Then, the whole state evolves to

$$|\Psi\rangle_5 = \frac{1}{\sqrt{2}}[\mathrm{e}^{\mathrm{i}\varphi}\mu(|R\rangle_{L_0,L,b}|+\rangle_1|+\rangle_2 + |L\rangle_{L_1,L,a}|-\rangle_1|-\rangle_2) + \mathrm{e}^{\mathrm{i}\omega}\nu(|R\rangle_{L_0,L,a}|+\rangle_1|+\rangle_2 + |L\rangle_{L_1,L,b}|-\rangle_1|-\rangle_2)]|+\rangle_3|+\rangle_4, \tag{12}$$

after the photon pulse goes through $\rm PBS_3$, $\rm S_5$–$\rm S_8$. Immediately following, the photon pulse will go through $\rm PBS_4$–$\rm PBS_8$ and the system state is transformed to

$$\begin{aligned} |\Psi\rangle_6 = \frac{1}{\sqrt{2}}&[\mathrm{e}^{\mathrm{i}\varphi}\mu(|R\rangle_{L_0,L,c,L_1}|+\rangle_1|+\rangle_2 + |L\rangle_{L_1,L,c,L_0}|-\rangle_1|-\rangle_2) \\ &+\mathrm{e}^{\mathrm{i}\omega}\nu(|R\rangle_{L_0,L,d,L_1}|+\rangle_1|+\rangle_2 + |L\rangle_{L_1,L,d,L_0})|-\rangle_1|-\rangle_2]|+\rangle_3|+\rangle_4. \end{aligned} \tag{13}$$

From Eq. (13), we can see that photons in path c or d are by far synchronized because the effective path length they passed are both equal to $L_0 + L_1 + L$. After the subsequent delay line $L_{\rm D}$ in path d, optical switch $\rm S_9$, $\rm PBS_9$, $\rm NV_3$, and $\rm NV_4$ work, and the state of the system evolves to

$$\begin{aligned} |\Psi\rangle_7 = &\frac{\mathrm{e}^{\mathrm{i}\varphi}\mu}{\sqrt{2}}(|R\rangle_{L_0,L,L_1,e}|+\rangle_1|+\rangle_2|+\rangle_3|+\rangle_4 \\ &+|L\rangle_{L_1,L,L_0,f}|-\rangle_1|-\rangle_2|-\rangle_3|-\rangle_4) \\ &+\frac{\mathrm{e}^{\mathrm{i}\omega}\nu}{\sqrt{2}}(|R\rangle_{L_0,L,L_1,L_{\rm D},e}|+\rangle_1|+\rangle_2|+\rangle_3|+\rangle_4 \end{aligned}$$

$$+|L\rangle_{L_1,L,L_0,L_D,f}|-\rangle_1|-\rangle_2|-\rangle_3|-\rangle_4). \quad (14)$$

Then, the photon pulse in paths e and f will be delivered into path g and h through a 50:50 beam splitter, whose function could be expressed as[74]

$$|R\rangle_e = (|R\rangle_g + |R\rangle_h)/\sqrt{2}; \quad |R\rangle_f = (|R\rangle_g - |R\rangle_h)/\sqrt{2};$$
$$|L\rangle_e = (|L\rangle_g + |L\rangle_h)/\sqrt{2}; \quad |L\rangle_f = (|L\rangle_g - |L\rangle_h)/\sqrt{2}. \quad (15)$$

And after the photon pulse passes through HWP_5 and HWP_6, the relevant system state is converted into

$$\begin{aligned}|\Psi\rangle_8 = {} & \frac{e^{i\varphi}\mu}{2}(|R\rangle_{L_0,L,L_1,D_1}|GHZ\rangle_1 + |L\rangle_{L_0,L,L_1,D_2}|GHZ\rangle_2 \\ & + |R\rangle_{L_0,L,L_1,D_3}|GHZ\rangle_2 + |L\rangle_{L_0,L,L_1,D_4}|GHZ\rangle_1) \\ & + \frac{e^{i\omega}\nu}{2}(|R\rangle_{L_0,L,L_1,L_D,D_1}|GHZ\rangle_1 \\ & + |L\rangle_{L_0,L,L_1,L_D,D_2}|GHZ\rangle_2 + |R\rangle_{L_0,L,L_1,L_D,D_3}|GHZ\rangle_2 \\ & + |L\rangle_{L_0,L,L_1,L_D,D_4}|GHZ\rangle_1), \end{aligned} \quad (16)$$

in which

$$|GHZ\rangle_1 = (|+\rangle_1|+\rangle_2|+\rangle_3|+\rangle_4 + |-\rangle_1|-\rangle_2|-\rangle_3|-\rangle_4)/\sqrt{2}$$

and

$$|GHZ\rangle_2 = (|+\rangle_1|+\rangle_2|+\rangle_3|+\rangle_4 - |-\rangle_1|-\rangle_2|-\rangle_3|-\rangle_4)/\sqrt{2},$$

and subscripts D_i ($i = 1, 2, 3, 4$) of the polarization state mean that this polarization state will be detected by the detector D_i. From Eq. (16), we can see the following results. (i) The phase noise produced in channel has no influence on the state generation because it has been converted to a collective phase which has no observable effects. (ii) Polarization noise μ and ν can influence the time of the desired state generation rather than the success probability and fidelity of the state generation because the state would be transformed to the maximum entangled GHZ state after any one of the four detectors clicks at the time $(L_0 + L_1 + L)/c$ or $(L_0 + L_1 + L + L_D)/c$. If detector D_1 clicks at time $(L_0 + L_1 + L)/c$, then the system state will collapse to state $|GHZ\rangle_1$, while if detector D_2 clicks at time $(L_0 + L_1 + L)/c$, then the system state will collapse to state $|GHZ\rangle_2$. The other six cases and the corresponding GHZ states could be achieved analogously.

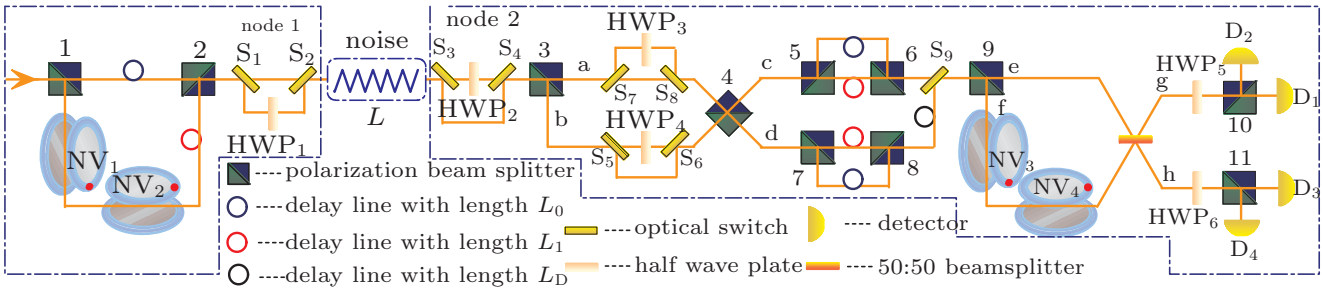


Fig. 2. (color online) A schematic diagram for GHZ state generation through noisy channel. Numbers 1–11 denote the polarization beam splitters (PBS), whose function is to translate R polarization light and reflect L polarization light. The role of the half wave plate 1 (HWP_1)–HWP_4 is to perform σ_x operation ($|R\rangle \leftrightarrow |L\rangle$) on photon state, while the function of HWP_5 and HWP_6 can be represented as $|R\rangle \rightarrow (|R\rangle + |L\rangle)/\sqrt{2}; |L\rangle \rightarrow (|R\rangle - |L\rangle)/\sqrt{2}$. The photon flying time difference between length L_0 and L_1 ($L_1 > L_0$) is big enough to make the optical switch transmit or reflect. Nevertheless, this time difference should be taken to be much less than the photon fluctuation time L/c in the noisy channel to ensure that the noise has the same effect on the photon coming from path L_0 or L_1. The action of L_D, which has a similar length to L_1, is to delay the photon pulse in the lower path. The lengths of paths without labelling L_0, L_1, L, and L_D are much less than $L_1 - L_0$ and can be ignored.

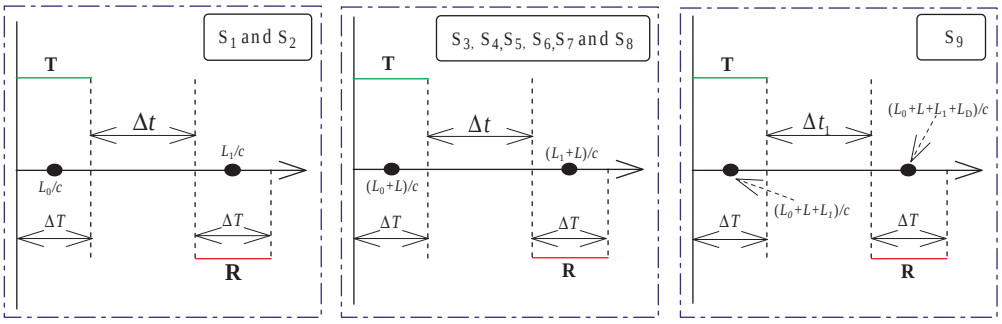


Fig. 3. (color online) Time control sequences of optical switches from S_1 to S_9. T and R mean that the optical switches are transmitted and reflected, respectively. ΔT is the photon pulse width, which should be far more less than the interval $(L_1 - L_0)/c$. Thus, $\Delta t \simeq (L_1 - L_0)/c$, and $\Delta t_1 \simeq L_D/c$. The time between S_3 and S_6 or between S_3 and S_8 should be much less than Δt and have been ignored.

3.2. W state

We now describe the process for four-qubit W state generation between two nodes. The sketch is shown in Fig. 4. The control sequences of optical switches are shown in Fig. 3. Assuming that the initial photon pulse is in state $|R\rangle$ and the four NV centers are all in state $|+\rangle$. Thus, the initial system state could be represented as

$$|\Phi\rangle_1 = |R\rangle|+\rangle_1|+\rangle_2|+\rangle_3|+\rangle_4, \tag{17}$$

which would be transformed to

$$|\Phi\rangle_2 = \frac{1}{2}|L\rangle|-\rangle_1|+\rangle_2|+\rangle_3|+\rangle_4 + \frac{1}{2}|L\rangle|+\rangle_1|-\rangle_2|+\rangle_3|+\rangle_4 + \frac{\sqrt{2}}{2}|R\rangle|+\rangle_1|+\rangle_2|+\rangle_3|+\rangle_4, \tag{18}$$

after HWP_1, NV_1, PBS_1, HWP_2, and NV_2 work. After the photon pulse passes through the time-bin encoding apparatus and optical switches S_1 and S_2, the system state will evolve to

$$|\Phi\rangle_3 = \frac{1}{2}|R\rangle_{L_1}|-\rangle_1|+\rangle_2|+\rangle_3|+\rangle_4 + \frac{1}{2}|R\rangle_{L_1}|+\rangle_1|-\rangle_2|+\rangle_3|+\rangle_4 + \frac{\sqrt{2}}{2}|R\rangle_{L_0}|+\rangle_1|+\rangle_2|+\rangle_3|+\rangle_4. \tag{19}$$

Suppose the influence on photon pulse induced by noisy channel is same as Eq. (9), and would change system state to

$$|\Phi\rangle_4 = \frac{1}{2}(\mathrm{e}^{\mathrm{i}\varphi}\mu|R\rangle + \mathrm{e}^{\mathrm{i}\omega}\nu|L\rangle)_{L_1,L}|-\rangle_1|+\rangle_2|+\rangle_3|+\rangle_4 + \frac{1}{2}(\mathrm{e}^{\mathrm{i}\varphi}\mu|R\rangle + \mathrm{e}^{\mathrm{i}\omega}\nu|L\rangle)_{L_1,L}|+\rangle_1|-\rangle_2|+\rangle_3|+\rangle_4 + \frac{\sqrt{2}}{2}(\mathrm{e}^{\mathrm{i}\varphi}\mu|R\rangle + \mathrm{e}^{\mathrm{i}\omega}\nu|L\rangle)_{L_0,L}|+\rangle_1|+\rangle_2|+\rangle_3|+\rangle_4. \tag{20}$$

Then from Fig. 4, the system has the following process

$$\xrightarrow{\mathrm{S}_3-\mathrm{S}_8,\mathrm{PBS}_5-\mathrm{PBS}_9} \frac{1}{2}(\mathrm{e}^{\mathrm{i}\varphi}\mu|L\rangle_{L_1,L,c,L_0} + \mathrm{e}^{\mathrm{i}\omega}\nu|L\rangle_{L_1,L,d,L_0})|-\rangle_1|+\rangle_2|+\rangle_3|+\rangle_4 + \frac{1}{2}(\mathrm{e}^{\mathrm{i}\varphi}\mu|L\rangle_{L_1,L,c,L_0} + \mathrm{e}^{\mathrm{i}\omega}\nu|L\rangle_{L_1,L,d,L_0})|+\rangle_1|-\rangle_2|+\rangle_3|+\rangle_4 + \frac{\sqrt{2}}{2}(\mathrm{e}^{\mathrm{i}\varphi}\mu|R\rangle_{L_0,L,c,L_1} + \mathrm{e}^{\mathrm{i}\omega}\nu|R\rangle_{L_0,L,d,L_1}) \times|+\rangle_1|+\rangle_2|+\rangle_3|+\rangle_4. \tag{21}$$

The component of the photon pulse in path d would go through an extra delay line L_D and the state would be transformed to

$$\begin{aligned}&\mathrm{e}^{\mathrm{i}\varphi}\mu\Big[\frac{1}{2}|L\rangle_{L_1,L,c,L_0}|-\rangle_1|+\rangle_2|+\rangle_3|+\rangle_4 + \frac{1}{2}|L\rangle_{L_1,L,c,L_0}|+\rangle_1|-\rangle_2|+\rangle_3|+\rangle_4 + \frac{\sqrt{2}}{2}|R\rangle_{L_0,L,c,L_1}|+\rangle_1|+\rangle_2|+\rangle_3|+\rangle_4\Big] \\ &+\mathrm{e}^{\mathrm{i}\omega}\nu[\frac{1}{2}|L\rangle_{L_1,L,d,L_0,L_\mathrm{D}}|-\rangle_1|+\rangle_2|+\rangle_3|+\rangle_4 + \frac{1}{2}|L\rangle_{L_1,L,d,L_0,L_\mathrm{D}}|+\rangle_1|-\rangle_2|+\rangle_3|+\rangle_4 + \frac{\sqrt{2}}{2}|R\rangle_{L_0,L,d,L_1,L_\mathrm{D}}|+\rangle_1|+\rangle_2|+\rangle_3|+\rangle_4]. \end{aligned} \tag{22}$$

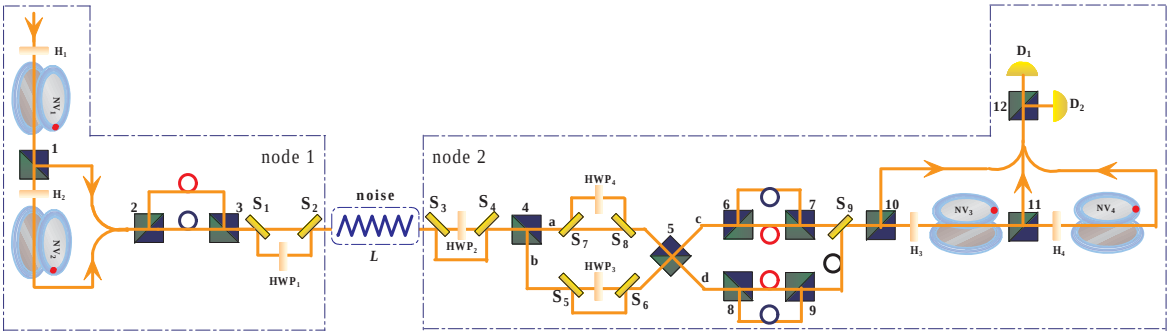


Fig. 4. (color online) A sketch of W state generation. H_1, H_2, H_3, and H_4 denote the HWP with the action $|R\rangle \to (|L\rangle + \sqrt{3}|R\rangle)/2$, $|R\rangle \to (|L\rangle + \sqrt{2}|R\rangle)/\sqrt{3}$, $|R\rangle \to (|L\rangle + |R\rangle)/\sqrt{2}$, and $|R\rangle \to |L\rangle$ on the photon pulse, respectively. The role of the HWP_1, HWP_2, HWP_3, HWP_4 is to perform a σ_x operation ($|R\rangle \leftrightarrow |L\rangle$) on the photon. The optical control sequences and requirement of delay lines are the same as GHZ state generation.

The system state will have the following evolving process after the photon pulse interacts with the rest devices

$$\begin{aligned}&\xrightarrow{\mathrm{S}_9,\ \mathrm{PBS}_{10},\ \mathrm{HWP}_7,\ \mathrm{NV}_3} \mathrm{e}^{\mathrm{i}\varphi}\mu\Big[\frac{1}{2}|L\rangle_{L_1,L,L_0}|-\rangle_1|+\rangle_2|+\rangle_3|+\rangle_4 + \frac{1}{2}|L\rangle_{L_1,L,L_0}|+\rangle_1|-\rangle_2|+\rangle_3|+\rangle_4 \\ &+\frac{1}{2}|L\rangle_{L_0,L,L_1}|+\rangle_1|+\rangle_2|-\rangle_3|+\rangle_4 + \frac{1}{2}|R\rangle_{L_0,L,L_1}|+\rangle_1|+\rangle_2|+\rangle_3|+\rangle_4\Big] \\ &+\mathrm{e}^{\mathrm{i}\omega}\nu\Big[\frac{1}{2}|L\rangle_{L_1,L,L_0,L_\mathrm{D}}|-\rangle_1|+\rangle_2|+\rangle_3|+\rangle_4 + \frac{1}{2}|L\rangle_{L_1,L,L_0,L_\mathrm{D}}|+\rangle_1|-\rangle_2|+\rangle_3|+\rangle_4 \\ &+\frac{1}{2}|L\rangle_{L_0,L,L_1,L_\mathrm{D}}|+\rangle_1|+\rangle_2|-\rangle_3|+\rangle_4 + \frac{1}{2}|R\rangle_{L_0,L,L_1,L_\mathrm{D}}|+\rangle_1|+\rangle_2|+\rangle_3|+\rangle_4\Big] \\ &\xrightarrow{\mathrm{PBS}_{11},\ \mathrm{HWP}_8,\ \mathrm{NV}_4} \frac{\mathrm{e}^{\mathrm{i}\varphi}\mu}{2}|L\rangle_{L_1,L,L_0,\mathrm{D}_2} \times[|-\rangle_1|+\rangle_2|+\rangle_3|+\rangle_4 + |+\rangle_1|-\rangle_2|+\rangle_3|+\rangle_4 \\ &+|+\rangle_1|+\rangle_2|-\rangle_3|+\rangle_4 + |+\rangle_1|+\rangle_2|+\rangle_3|-\rangle_4] \\ &+\frac{\mathrm{e}^{\mathrm{i}\omega}\nu}{2}|L\rangle_{L_1,L,L_0,L_\mathrm{D},\mathrm{D}_2} \times[|-\rangle_1|+\rangle_2|+\rangle_3|+\rangle_4 + |+\rangle_1|-\rangle_2|+\rangle_3|+\rangle_4\end{aligned}$$

$$+|+\rangle_1|+\rangle_2|-\rangle_3|+\rangle_4+|+\rangle_1|+\rangle_2|+\rangle_3|-\rangle_4]. \quad (23)$$

It is easy to see that the polarization noise and phase noise have no influence on the state generation. If detector D_2 clicks at time $(L_1+L+L_0)/c$ or $(L_1+L+L_0+L_D)/c$, then the state of the four NV centers would both collapse to W state determinately.

4. Generating *n*-Qubit entanglement among *n* nodes through regular noise-changeable channels

Next, we shift our attention to illustrate the principle for generalizing the above proposals to n-qubit among two nodes or n ($n \geqslant 3$) nodes. For the case of n ($n \geqslant 3$) nodes, the proposals are robust for the regular changeable noise. This merit enables our proposals to have broadened applications in large scale QIP through noisy channels.

4.1. GHZ state

In this subsection, we illustrate the process of n-qubit GHZ state generation among n nodes, which are schematically drawn in Fig. 5. The case to generate n-qubit GHZ states between two nodes can be easily derived by following the process in Subsection 3.1 by adding NV centers behind NV 2 or NV 4 in Fig. 2. Thus, we will focus on describing the n nodes case in this subsection.

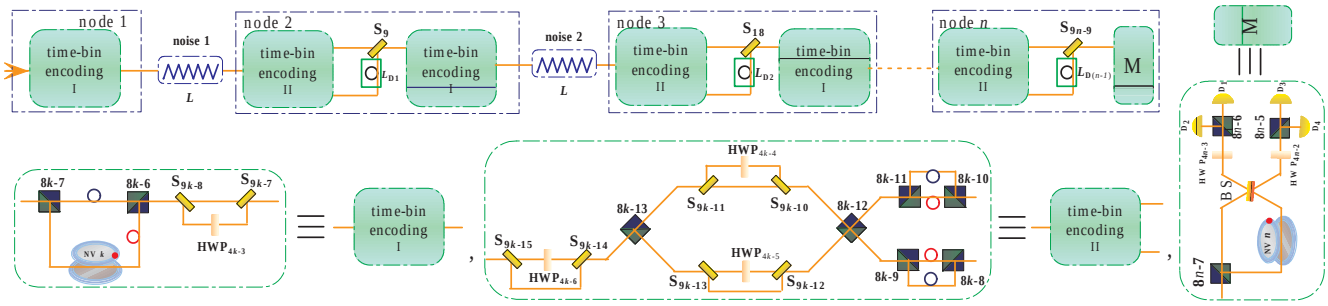


Fig. 5. (color online) A schematic diagram to generalize GHZ state generation to n-qubit case among n nodes. The role of HWP_1-HWP_{4n-4} is to perform a σ_x operation on the photon pulse, while the role of HWP_{4n-3} and HWP_{4n-2} is to realize the transformation $|R\rangle \to (|R\rangle+|L\rangle)/\sqrt{2}; |L\rangle \to (|R\rangle-|L\rangle)/\sqrt{2}$. The control sequences of optical switches are shown in Fig. 7. Subscript k denotes the sequence number of the node where the optical switches are located. It should be noted that the optical path and the elements from node 2 to node $n-1$ are all same, except the the delay lines (marked with green boxes) under the optical switches S_{9k-9}, whose length is designed as $L_{\mathrm{D}j} = 2^{j-1}L_{\mathrm{D}}$ $(1 \leqslant j \leqslant n-1)$.

We first consider the 3-node case, based on which the n-node case can be understood and derived. The initial state is $|\varphi\rangle_1 = (|R\rangle+|L\rangle)|+\rangle_1|+\rangle_2|+\rangle_3/\sqrt{2}$. Assuming that the noisy channel 1 has the effect $|R\rangle \xrightarrow{\text{noisy channel1}} \mathrm{e}^{\mathrm{i}\varphi_1}\mu_1|R\rangle + \mathrm{e}^{\mathrm{i}\omega_1}\nu_1|L\rangle$, and noisy channel 2 has the effect $|R\rangle \xrightarrow{\text{noisy channel 2}} \mathrm{e}^{\mathrm{i}\varphi_2'}\mu_2'|R\rangle + \mathrm{e}^{\mathrm{i}\omega_2'}\nu_2'|L\rangle$ on the pulse with arriving time inside interval $(2L_0+L_1+L)/c$–$(L_0+2L_1+L)/c$ and $|R\rangle \xrightarrow{\text{noisy channel 2}} \mathrm{e}^{\mathrm{i}\varphi_2''}\mu_2''|R\rangle + \mathrm{e}^{\mathrm{i}\omega_2''}\nu_2''|L\rangle$ on the pulse with arriving time inside interval $(2L_0+L_1+L+L_D)/c$–$(L_0+2L_1+L+L_D)/c$, respectively. The control sequences of optical switches S_1–S_9 and S_{10}–S_{18} are shown in Fig. 3 and Fig. 6, respectively. The state evolution process can be expressed as

$$\begin{aligned}
&|\varphi\rangle_1 \xrightarrow{\mathrm{PBS}_1,\ \mathrm{PBS}_2,\ \text{noisy channel 1}} \\
&\frac{1}{\sqrt{2}}[(\mathrm{e}^{\mathrm{i}\varphi_1}\mu_1|R\rangle + \mathrm{e}^{\mathrm{i}\omega_1}\nu_1|L\rangle)_{L_0,L}|+\rangle_1 \\
&+(\mathrm{e}^{\mathrm{i}\varphi_1}\mu_1|R\rangle + \mathrm{e}^{\mathrm{i}\omega_1}\nu_1|L\rangle)_{L_1,L}|-\rangle_1]|+\rangle_2|+\rangle_3 \\
&\xrightarrow{\text{all elements in node 2, noisy channel 2}} \\
&\frac{\mathrm{e}^{\mathrm{i}\varphi_1}\mu_1}{\sqrt{2}}[(\mathrm{e}^{\mathrm{i}\varphi_2'}\mu_2'|R\rangle + \mathrm{e}^{\mathrm{i}\omega_2'}\nu_2'|L\rangle)_{2L_0,L_1,2L}|+\rangle_1|+\rangle_2 \\
&+(\mathrm{e}^{\mathrm{i}\varphi_2'}\mu_2'|R\rangle + \mathrm{e}^{\mathrm{i}\omega_2'}\nu_2'|L\rangle)_{L_0,2L_1,2L}|-\rangle_1|-\rangle_2]|+\rangle_3 \\
&+\frac{\mathrm{e}^{\mathrm{i}\omega_1}\nu_1}{\sqrt{2}}[(\mathrm{e}^{\mathrm{i}\varphi_2''}\mu_2''|R\rangle + \mathrm{e}^{\mathrm{i}\omega_2''}\nu_2''|L\rangle)_{2L_0,L_1,2L,L_D}|+\rangle_1|+\rangle_2 \\
&+(\mathrm{e}^{\mathrm{i}\varphi_2''}\mu_2''|R\rangle + \mathrm{e}^{\mathrm{i}\omega_2''}\nu_2''|L\rangle)_{L_0,2L_1,2L,L_D}|-\rangle_1|-\rangle_2]|+\rangle_3 \\
&\xrightarrow{\text{all elements in node 3 (except detectors)}} \\
&\frac{\mathrm{e}^{\mathrm{i}\varphi_1}\mu_1}{2}[\mathrm{e}^{\mathrm{i}\varphi_2'}\mu_2'(|R\rangle_{2L_0,2L_1,2L,\mathrm{D}_1}|GHZ\rangle_+ \\
&+|L\rangle_{2L_0,2L_1,2L,\mathrm{D}_2}|GHZ\rangle_- + |R\rangle_{2L_0,2L_1,2L,\mathrm{D}_3}|GHZ\rangle_- \\
&+|L\rangle_{2L_0,2L_1,2L,\mathrm{D}_4}|GHZ\rangle_+) \\
&+\mathrm{e}^{\mathrm{i}\omega_2'}\nu_2'(|R\rangle_{2L_0,2L_1,2L,2L_D,\mathrm{D}_1}|GHZ\rangle_+ \\
&+|L\rangle_{2L_0,2L_1,2L,2L_D,\mathrm{D}_2}|GHZ\rangle_- + |R\rangle_{2L_0,2L_1,2L,2L_D,\mathrm{D}_3}|GHZ\rangle_- \\
&+|L\rangle_{2L_0,2L_1,2L,2L_D,\mathrm{D}_4}|GHZ\rangle_+)] \\
&+\frac{\mathrm{e}^{\mathrm{i}\omega_1}\nu_1}{2}[\mathrm{e}^{\mathrm{i}\varphi_2''}\mu_2''(|R\rangle_{2L_0,2L_1,2L,L_D,\mathrm{D}_1}|GHZ\rangle_+ \\
&+|L\rangle_{2L_0,2L_1,2L,L_D,\mathrm{D}_2}|GHZ\rangle_- + |R\rangle_{2L_0,2L_1,2L,L_D,\mathrm{D}_3}|GHZ\rangle_- \\
&+|L\rangle_{2L_0,2L_1,2L,L_D,\mathrm{D}_4}|GHZ\rangle_+) \\
&+\mathrm{e}^{\mathrm{i}\omega_2''}\nu_2''(|R\rangle_{2L_0,2L_1,2L,3L_D,\mathrm{D}_1}|GHZ\rangle_+ \\
&+|L\rangle_{2L_0,2L_1,2L,3L_D,\mathrm{D}_2}|GHZ\rangle_- + |R\rangle_{2L_0,2L_1,2L,3L_D,\mathrm{D}_3}|GHZ\rangle_- \\
&+|L\rangle_{2L_0,2L_1,2L,3L_D,\mathrm{D}_4}|GHZ\rangle_+)], \qquad (24)
\end{aligned}$$

where $|GHZ\rangle_+ = (|+\rangle_1|+\rangle_2|+\rangle_3 + |-\rangle_1|-\rangle_2|-\rangle_3)/\sqrt{2}$ and $|GHZ\rangle_- = (|+\rangle_1|+\rangle_2|+\rangle_3 - |-\rangle_1|-\rangle_2|-\rangle_3)/\sqrt{2}$. From the

above expression (24), we can obtain the following information, that is, a $|GHZ\rangle_+(|GHZ\rangle_-)$ state will be achieved if the detector D_1 or D_4 (D_2 or D_3) clicks at any one of the four following times, i.e., $(2L_0+2L_1+2L)/c$, $(2L_0+2L_1+2L+L_D)/c$, $(2L_0+2L_1+2L+2L_D)/c$, and $(2L_0+2L_1+2L+3L_D)/c$. That is to say, the steady noise introduced by the noisy channel 1 and the regular changeable noise introduced by the noisy channel 2 have no effect on the state generation.

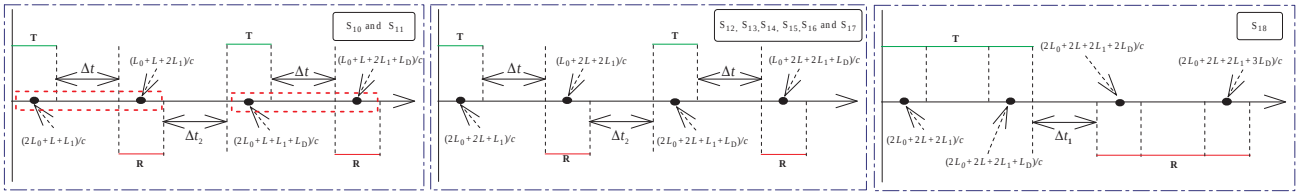


Fig. 6. (color online) Control sequences of optical switches S_{10}–S_{18}. The channels following optical switch S_{11} should have the same influence on the photon with arriving time inside the red-dotted-line-formed rectangle, but can have a different influence on the photon with arriving time inside a different red-dotted-line-formed rectangle. The control sequences of optical switches S_1–S_9 are identical to Fig. 3. $\Delta t_2 \backsimeq (L_D+L_0-L_1)/c$.

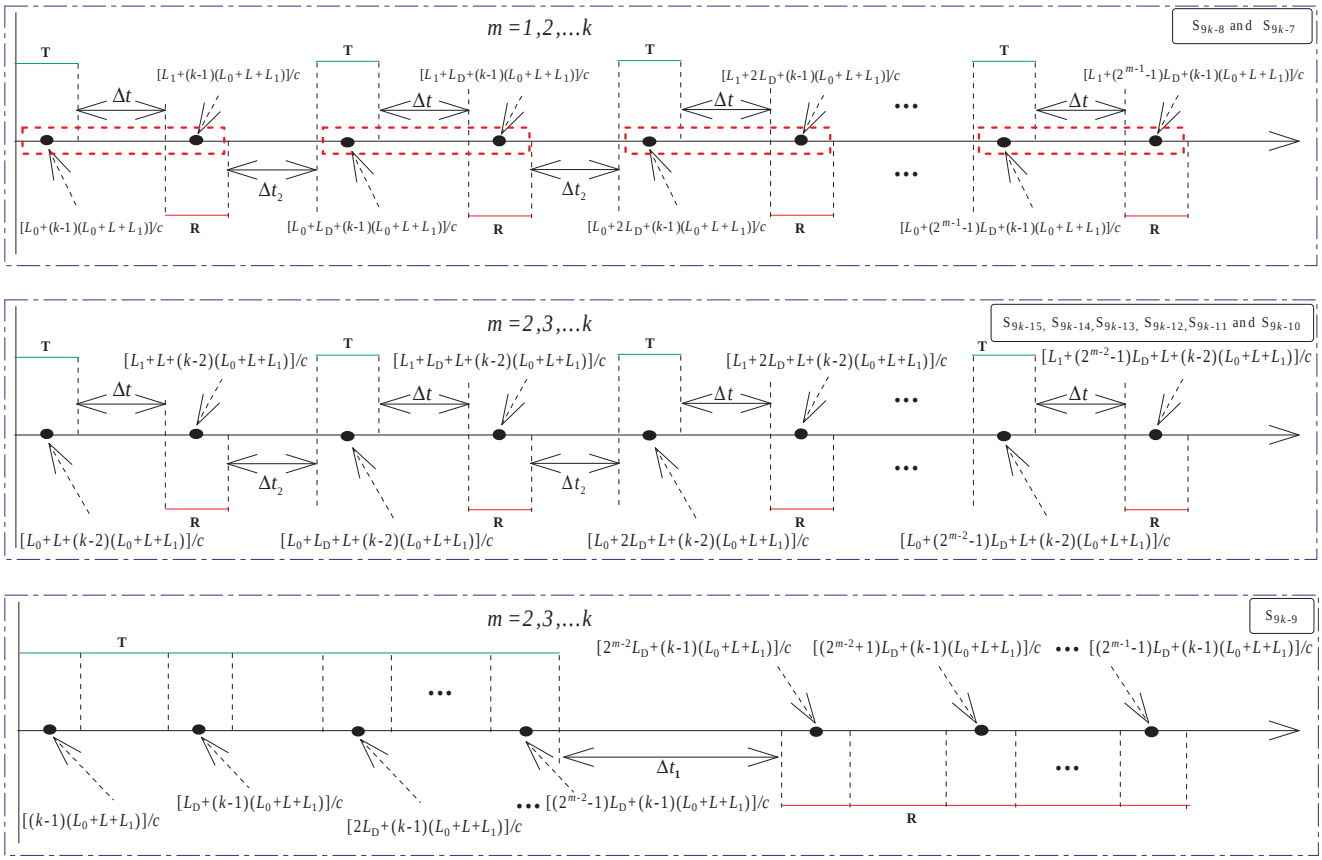


Fig. 7. (color online) Time control sequences of optical switches for n-node ($n \geqslant 3$) GHZ and W states generation. The regular noise-changeable channels following optical switch S_{9k-7} should have the same influence on the photon with arriving time inside the red-dotted-line-formed rectangle but can have a different influence on the photon with arriving time inside a different red-dotted-line-formed rectangle.

We now discuss the n-node ($n>3$) case. For simplicity, we assume that the noises in different channels are the same and can be expressed as $|R\rangle \to e^{i\varphi}\mu|R\rangle + e^{i\omega}\nu|L\rangle$. Initially, suppose that the photon pulse is in state $(|R\rangle+|L\rangle)/\sqrt{2}$, and each of the NV centers is in state $|+\rangle$. According to Fig. 5 and Fig. 7, the process of state evolution could be written as

$$\frac{1}{\sqrt{2}}(|R\rangle+|L\rangle)\otimes\prod_{i=1}^{n}|+\rangle_i \xrightarrow{\text{PBS}_1,\ \text{PBS}_2,\ \text{noisy channel 1}}$$

$$\frac{1}{\sqrt{2}}[(e^{i\varphi}\mu|R\rangle+e^{i\omega}\nu|L\rangle)_{L_0,L}|+\rangle_1+(e^{i\varphi}\mu|R\rangle+e^{i\omega}\nu|L\rangle)_{L_1,L}|-\rangle_1]\otimes\prod_{i=2}^{n}|+\rangle_i$$

$$\xrightarrow{\text{all elements in node 2, noisy channel 2}}$$

$$\frac{e^{i\varphi}\mu}{\sqrt{2}}[(e^{i\varphi}\mu|R\rangle+e^{i\omega}\nu|L\rangle)_{2L_0,L_1,2L}|+\rangle_1|+\rangle_2+(e^{i\varphi}\mu|R\rangle+e^{i\omega}\nu|L\rangle)_{L_0,2L_1,2L}|-\rangle_1|-\rangle_2]\otimes\prod_{i=3}^{n}|+\rangle_i$$

$$+\frac{e^{i\omega}\nu}{\sqrt{2}}[(e^{i\varphi}\mu|R\rangle+e^{i\omega}\nu|L\rangle)_{2L_0,L_1,2L,L_D}|+\rangle_1|+\rangle_2+(e^{i\varphi}\mu|R\rangle+e^{i\omega}\nu|L\rangle)_{L_0,2L_1,2L,L_D}|-\rangle_1|-\rangle_2]\otimes\prod_{i=3}^{n}|+\rangle_i$$

$$\xrightarrow{\text{all elements in node 3, noisy channel 3}}$$

$$\frac{(e^{i\varphi}\mu)^2}{\sqrt{2}}\left[(e^{i\varphi}\mu|R\rangle+e^{i\omega}\nu|L\rangle)_{3L_0,2L_1,3L}\prod_{j=1}^{3}|+\rangle_j+(e^{i\varphi}\mu|R\rangle+e^{i\omega}\nu|L\rangle)_{2L_0,3L_1,3L}\prod_{j=1}^{3}|-\rangle_j\right]\otimes\prod_{i=4}^{n}|+\rangle_i$$

$$+\frac{e^{i\omega}\nu e^{i\varphi}\mu}{\sqrt{2}}\left[(e^{i\varphi}\mu|R\rangle+e^{i\omega}\nu|L\rangle)_{3L_0,2L_1,3L,2L_D}\prod_{j=1}^{3}|+\rangle_j+(e^{i\varphi}\mu|R\rangle+e^{i\omega}\nu|L\rangle)_{2L_0,3L_1,3L,2L_D}\prod_{j=1}^{3}|-\rangle_j\right]\otimes\prod_{i=4}^{n}|+\rangle_i$$

$$+\frac{e^{i\varphi}\mu e^{i\omega}\nu}{\sqrt{2}}\left[(e^{i\varphi}\mu|R\rangle+e^{i\omega}\nu|L\rangle)_{3L_0,2L_1,3L,L_D}\prod_{j=1}^{3}|+\rangle_j+(e^{i\varphi}\mu|R\rangle+e^{i\omega}\nu|L\rangle)_{2L_0,3L_1,3L,L_D}\prod_{j=1}^{3}|-\rangle_j\right]\otimes\prod_{i=4}^{n}|+\rangle_i$$

$$+\frac{(e^{i\omega}\nu)^2}{\sqrt{2}}\left[(e^{i\varphi}\mu|R\rangle+e^{i\omega}\nu|L\rangle)_{3L_0,2L_1,3L,3L_D}\prod_{j=1}^{3}|+\rangle_j+(e^{i\varphi}\mu|R\rangle+e^{i\omega}\nu|L\rangle)_{2L_0,3L_1,3L,3L_D}\prod_{j=1}^{3}|-\rangle_j\right]\otimes\prod_{i=4}^{n}|+\rangle_i$$

$$\xrightarrow{\cdots}\cdots$$

$$\xrightarrow{\text{all elements in node }(n-1)\text{, noisy channel }(n-1)}\frac{(e^{i\varphi}\mu)^{n-2}}{\sqrt{2}}\left[(e^{i\varphi}\mu|R\rangle+e^{i\omega}\nu|L\rangle)_{(n-1)L_0,(n-2)L_1,(n-1)L}\prod_{j=1}^{n-1}|+\rangle_j\right.$$

$$\left.+(e^{i\varphi}\mu|R\rangle+e^{i\omega}\nu|L\rangle)_{(n-2)L_0,(n-1)L_1,(n-1)L}\prod_{j=1}^{n-1}|-\rangle_j\right]\otimes|+\rangle_n\cdots$$

$$+\frac{(e^{i\omega}\nu)^{n-2}}{\sqrt{2}}\left[(e^{i\varphi}\mu|R\rangle+e^{i\omega}\nu|L\rangle)_{(n-1)L_0,(n-2)L_1,(n-1)L,(2^{n-2}-1)L_D}\prod_{j=1}^{n-1}|+\rangle_n\right.$$

$$\left.+(e^{i\varphi}\mu|R\rangle+e^{i\omega}\nu|L\rangle)_{(n-2)L_0,(n-1)L_1,(n-1)L,(2^{n-2}-1)L_D}\prod_{j=1}^{n-1}|-\rangle_j\right]\otimes|+\rangle_n$$

$$\xrightarrow{\text{all elements in node }n\text{, (except detectors)}}\frac{(e^{i\varphi}\mu)^{n-1}}{2}\left[|R\rangle_{(n-1)L_0,(n-1)L_1,(n-1)L,D_1}\left(\prod_{j=1}^{n}|+\rangle_j+\prod_{j=1}^{n}|-\rangle_j\right)/\sqrt{2}\right.$$

$$+|L\rangle_{(n-1)L_0,(n-1)L_1,(n-1)L,D_2}\left(\prod_{j=1}^{n}|+\rangle_j-\prod_{j=1}^{n}|-\rangle_j\right)/\sqrt{2}+|R\rangle_{(n-1)L_0,(n-1)L_1,(n-1)L,D_3}\left(\prod_{j=1}^{n}|+\rangle_j-\prod_{j=1}^{n}|-\rangle_j\right)/\sqrt{2}$$

$$\left.+|L\rangle_{(n-1)L_0,(n-1)L_1,(n-1)L,D_4}\left(\prod_{j=1}^{n}|+\rangle_j+\prod_{j=1}^{n}|-\rangle_j\right)/\sqrt{2}\right]$$

$$+\frac{(e^{i\varphi}\mu)^{n-2}e^{i\omega}\nu}{2}[|R\rangle_{(n-1)L_0,(n-1)L_1,(n-1)L,2^{n-2}L_D,D_1}\left(\prod_{j=1}^{n}|+\rangle_j+\prod_{j=1}^{n}|-\rangle_j\right)/\sqrt{2}$$

$$+|L\rangle_{(n-1)L_0,(n-1)L_1,(n-1)L,2^{n-2}L_D,D_2}\left(\prod_{j=1}^{n}|+\rangle_j-\prod_{j=1}^{n}|-\rangle_j\right)/\sqrt{2}+|R\rangle_{(n-1)L_0,(n-1)L_1,(n-1)L,2^{n-2}L_D,D_3}\left(\prod_{j=1}^{n}|+\rangle_j-\prod_{j=1}^{n}|-\rangle_j\right)/\sqrt{2}$$

$$\left.+|L\rangle_{(n-1)L_0,(n-1)L_1,(n-1)L,2^{n-2}L_D,D_4}\left(\prod_{j=1}^{n}|+\rangle_j+\prod_{j=1}^{n}|-\rangle_j\right)/\sqrt{2}\right]\cdots$$

$$+\frac{(e^{i\omega}\nu)^{n-2}e^{i\varphi}\mu}{\sqrt{2}}[|R\rangle_{(n-1)L_0,(n-1)L_1,(n-1)L,(2^{n-2}-1)L_D,D_1}(\prod_{j=1}^{n}|+\rangle_j+\prod_{j=1}^{n}|-\rangle_j)/\sqrt{2}$$

$$+|L\rangle_{(n-1)L_0,(n-1)L_1,(n-1)L,(2^{n-2}-1)L_D,D_2}\left(\prod_{j=1}^{n}|+\rangle_j-\prod_{j=1}^{n}|-\rangle_j\right)/\sqrt{2}$$

$$+|R\rangle_{(n-1)L_0,(n-1)L_1,(n-1)L,(2^{n-2}-1)L_D,D_3}\left(\prod_{j=1}^{n}|+\rangle_j-\prod_{j=1}^{n}|-\rangle_j\right)/\sqrt{2}$$

$$+|L\rangle_{(n-1)L_0,(n-1)L_1,(n-1)L,(2^{n-2}-1)L_D,D_4}\left(\prod_{j=1}^{n}|+\rangle_j+\prod_{j=1}^{n}|-\rangle_j\right)/\sqrt{2}]$$

$$+\frac{(e^{i\omega}\nu)^{n-1}}{\sqrt{2}}[|R\rangle_{(n-1)L_0,(n-1)L_1,(n-1)L,(2^{n-1}-1)L_D,D_1}(\prod_{j=1}^{n}|+\rangle_j+\prod_{j=1}^{n}|-\rangle_j)/\sqrt{2}$$

$$+|L\rangle_{(n-1)L_0,(n-1)L_1,(n-1)L,(2^{n-1}-1)L_{\rm D},{\rm D}_2}\left(\prod_{j=1}^{n}|+\rangle_j-\prod_{j=1}^{n}|-\rangle_j\right)/\sqrt{2}$$
$$+|R\rangle_{(n-1)L_0,(n-1)L_1,(n-1)L,(2^{n-1}-1)L_{\rm D},{\rm D}_3}\left(\prod_{j=1}^{n}|+\rangle_j-\prod_{j=1}^{n}|-\rangle_j\right)/\sqrt{2}$$
$$+|L\rangle_{(n-1)L_0,(n-1)L_1,(n-1)L,(2^{n-1}-1)L_{\rm D},{\rm D}_4}\left(\prod_{j=1}^{n}|+\rangle_j+\prod_{j=1}^{n}|-\rangle_j\right)/\sqrt{2}\Big]. \tag{25}$$

From the last term in Eq. (25), one can see that if D_4 clicks at the time $[(n-1)L_0+(n-1)L_1+(n-1)L+(2^{n-1}-1)L_{\rm D}]/c$, then the n-qubit GHZ state $(\prod_{j=1}^{n}|+\rangle_j+\prod_{j=1}^{n}|-\rangle_j)/\sqrt{2}$ would be generated. Similar results would be achieved if other detectors click at the time $[(n-1)L_0+(n-1)L_1+(n-1)L+\ell L_{\rm D}]/c$ (ℓ is an integer which belongs to the interval $[0,(2^{n-1}-1)]$).

4.2. W state

The case of the n-qubit W state is schematically drawn in Fig. 8. The case to generate a n-qubit W state between two nodes can be derived similarly according to Subsection 3.2 and Fig. 8(a). Thus, we focus on the case among n nodes. For simplicity, we first consider the three-node case, based on which the n-node case can be deduced. The initial state of the whole system is $|\psi\rangle_1=|R\rangle|+\rangle_1|+\rangle_2|+\rangle_3$. Assuming that the influence of noisy channels is the same as in Subsection 4.1, then we can have the following process

$$\begin{aligned}
&|\psi\rangle_1 \xrightarrow{\text{all elements in node 1, noisy channel 1}}\\
&\frac{1}{\sqrt{3}}[(e^{i\varphi_1}\mu_1|R\rangle+e^{i\omega_1}\nu_1|L\rangle)_{L_1,L}|-\rangle_1\\
&+\sqrt{2}(e^{i\varphi_1}\mu_1|R\rangle+e^{i\omega_1}\nu_1|L\rangle)_{L_0,L}|+\rangle_1]|+\rangle_2|+\rangle_3.\\
&\xrightarrow{\text{all elements in node 2, noisy channel 2}}\\
&\frac{1}{\sqrt{3}}[e^{i\varphi_1\mu_1}\big((e^{i\varphi_2'\mu_2'}|R\rangle+e^{i\omega_2'\nu_2'}|L\rangle)_{L_0,2L_1,2L}\\
&\otimes(|-\rangle_1|+\rangle_2+|+\rangle_1|-\rangle_2)\\
&+(e^{i\varphi_2'\mu_2'}|R\rangle+e^{i\omega_2'\nu_2'}|L\rangle)_{2L_0,L_1,2L}|+\rangle_1|+\rangle_2\big)\\
&+e^{i\omega_1\nu_1}\big((e^{i\varphi_2''\mu_2''}|R\rangle+e^{i\omega_2''\nu_2''}|L\rangle)_{L_0,2L_1,2L,L_{\rm D}}\\
&\otimes(|-\rangle_1|+\rangle_2+|+\rangle_1|-\rangle_2)\\
&+(e^{i\varphi_2''\mu_2''}|R\rangle+e^{i\omega_2''\nu_2''}|L\rangle)_{2L_0,L_1,2L,L_{\rm D}}|+\rangle_1|+\rangle_2\big)\big]|+\rangle_3\\
&\xrightarrow{\text{all elements in node 3 (except detectors)}}\\
&\frac{1}{\sqrt{3}}[e^{i\varphi_1}\mu_1\big(e^{i\varphi_2'}\mu_2'|L\rangle_{2L_0,2L_1,2L}(|-\rangle_1|+\rangle_2|+\rangle_3\\
&+|+\rangle_1|-\rangle_2|+\rangle_3+|+\rangle_1|+\rangle_2|-\rangle_3)\\
&+e^{i\omega_2'}\nu_2'|L\rangle_{2L_0,2L_1,2L,2L_{\rm D}}(|-\rangle_1|+\rangle_2|+\rangle_3\\
&+|+\rangle_1|-\rangle_2|+\rangle_3+|+\rangle_1|+\rangle_2|-\rangle_3)\big)\\
&+e^{i\omega_1}\nu_1\big(e^{i\varphi_2''}\mu_2|L\rangle_{2L_0,2L_1,2L,L_{\rm D}}(|-\rangle_1|+\rangle_2|+\rangle_3\\
&+|+\rangle_1|-\rangle_2|+\rangle_3+|+\rangle_1|+\rangle_2|-\rangle_3)\\
&+e^{i\omega_2''}\nu_2''|L\rangle_{2L_0,2L_1,2L,3L_{\rm D}}(|-\rangle_1|+\rangle_2|+\rangle_3\\
&+|+\rangle_1|-\rangle_2|+\rangle_3+|+\rangle_1|+\rangle_2|-\rangle_3)\big)].
\end{aligned}\tag{26}$$

From Eq. (26), we can see that the steady noise caused by channel 1 and the regular changeable noise caused by channel 2 would influence the time of state generation but have no effect on the success probability and fidelity. The n-node case can also be derived in a similar way based on the sketch in Fig. 8(b) and the control sequences of the optical switches in Fig. 7.

We now discuss the n-node ($n>3$) case. For simplicity, supposing that the noises in different channels are the same and can be expressed as $|R\rangle\to e^{i\varphi}\mu|R\rangle+e^{i\omega}\nu|L\rangle$. Initially, the photon pulse is in state $|R\rangle$, and each of the NV centers is in state $|+\rangle$. According to Fig. 7 and Fig. 8, the process of state evolution could be written as

$$\begin{aligned}
&|R\rangle\otimes\prod_{i=1}^{n}|+\rangle_i\\
&\xrightarrow{\text{all elements in node 1, noisy channel 1}}\\
&\frac{1}{\sqrt{n}}[(e^{i\varphi}\mu|R\rangle+e^{i\omega}\nu|L\rangle)_{L_1,L}|-\rangle_1\\
&+\sqrt{n-1}(e^{i\varphi}\mu|R\rangle+e^{i\omega}\nu|L\rangle)_{L_0,L}|+\rangle_1]\prod_{i=2}^{n}|+\rangle_i\\
&\xrightarrow{\text{all elements in node 2, noisy channel 2}}\\
&\frac{1}{\sqrt{n}}[e^{i\varphi\mu}\big((e^{i\varphi\mu}|R\rangle+e^{i\omega\nu}|L\rangle)_{L_0,2L_1,2L}\\
&\otimes(|-\rangle_1|+\rangle_2+|+\rangle_1|-\rangle_2)\\
&+\sqrt{n-2}(e^{i\varphi\mu}|R\rangle+e^{i\omega\nu}|L\rangle)_{2L_0,L_1,2L}|+\rangle_1|+\rangle_2\big)\\
&+e^{i\omega\nu}\big((e^{i\varphi\mu}|R\rangle+e^{i\omega\nu}|L\rangle)_{L_0,2L_1,2L,L_{\rm D}}\\
&\otimes(|-\rangle_1|+\rangle_2+|+\rangle_1|-\rangle_2)\\
&+\sqrt{n-2}(e^{i\varphi\mu}|R\rangle+e^{i\omega\nu}|L\rangle)_{2L_0,L_1,2L,L_{\rm D}}|+\rangle_1|+\rangle_2)\big]\prod_{i=3}^{n}|+\rangle_i\\
&\xrightarrow{\cdots}\cdots\\
&\xrightarrow{\text{all elements in node } n \text{ (except detectors)}}\\
&\frac{1}{\sqrt{n}}[(e^{i\varphi}\mu)^{n-1}|L\rangle_{(n-1)L_0,(n-1)L_1,(n-1)L}\\
&\times\sum_{i=1}^{n}|+\rangle_1|+\rangle_2\otimes\cdots\otimes|-\rangle_i\otimes\cdots\otimes|+\rangle_{n-1}|+\rangle_n\\
&\cdots\\
&+(e^{i\omega}\nu)^{n-1}|L\rangle_{2L_0,2L_1,2L,(2^{n-1}-1)L_{\rm D}}\\
&\times\sum_{i=1}^{n}|+\rangle_1|+\rangle_2\otimes\cdots\otimes|-\rangle_i\otimes\cdots\otimes|+\rangle_{n-1}|+\rangle_n].
\end{aligned}\tag{27}$$

From Eq. (27), one can see that the n-qubit W state can be generated if detector D_2 clicks at any one of the times

$[(n-1)L_0+(n-1)L_1+(n-1)L+\ell L_D]/c$ (ℓ is an integer which belongs to the interval $[0,(2^{n-1}-1)]$). Moreover, the noises have no influence on state generation since the overall phase could be eliminated.

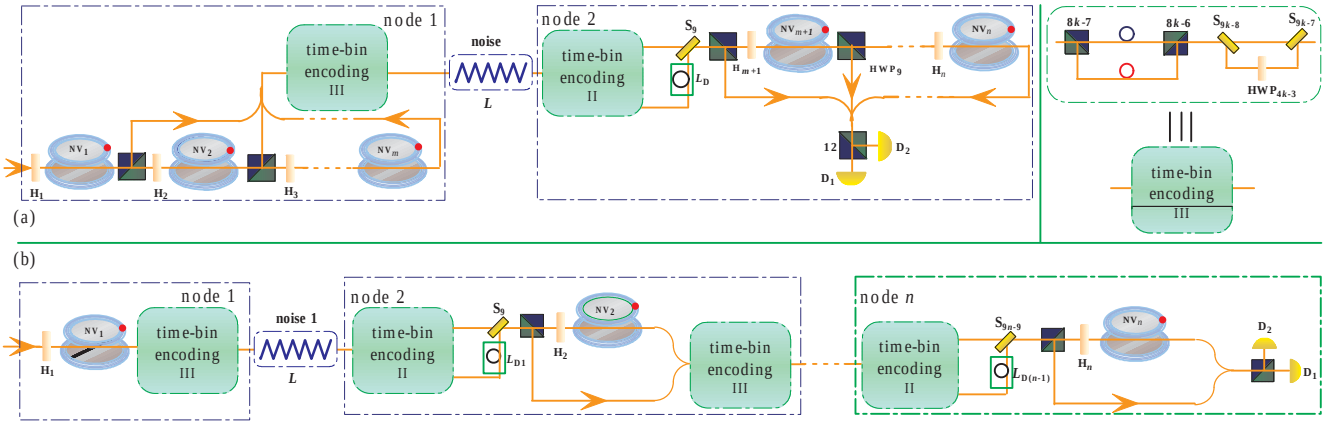


Fig. 8. (color online) A schematic diagram to generalize W state generation to n-qubit case. The photon pulses are both prepared in $|R\rangle$ state and the NV centers are all prepared in $|+\rangle$ state. H_l denotes the HWP with the action $|R\rangle \xrightarrow{H_l} \frac{1}{\sqrt{n-l+1}}|L\rangle+\frac{\sqrt{n-l}}{\sqrt{n-l+1}}|R\rangle$ $(1\leqslant l\leqslant n)$ and HWP_k denotes the HWP with the action $|R\rangle\leftrightarrow|L\rangle$. (a) To generate n qubit W state between two nodes. The control sequences are the same as those in Fig. 3. (b) To generate an n qubit W state among n nodes. The control sequences are the same as those in Fig. 6. The optical path and elements from node 2 to node $n-1$ are all the same, except for the delay lines (marked with green boxes) under the optical switches S_{9k-9}, whose length is designed as $L_{Dj}=2^{j-1}L_D$.

5. Discussion and conclusion

The feasibility of our proposals mainly depends on the time-bin encoding and the performance of our NV center, it is thus essential to discuss the experimental feasibility of these two primary components. The accuracy of the time is seriously dependent on the length of the delay lines. Thus, the delay line lengths L_0, L_1, and L_D are critical in our proposals. The time Δt, Δt_1, and Δt_2 should be big enough to make sure that the status of optical switches has enough time to be changed, which can be achieved by adjusting the lengths of L_0, L_1, and L_D. Meanwhile, the time interval Δt should be less than L/c to ensure that the noisy channel has a steady influence on the photon pulse with arriving time inside the red-dotted-line-formed rectangle, as shown in Fig. 7. In addition, L_D should have a similar value as L_1 to ensure $L_0+L_D>L_1$, this is the prerequisite condition to unmix the pulses with different noises and arriving times. In addition, The reason why we have not considered the interaction time between photon pulses and NV centers is that it has a smaller level. Sometimes it may even be bigger than $(L_1-L_0)/c$. Since the $|L\rangle$ component of photon pulse with different noises and arriving time will inevitably interact with the NV centers, we can add extra delay lines in the paths which $|R\rangle$ component passes through to make the two paths balanced. The only influence of these balanced paths is to shift the control sequences in Fig. 7 to the right for some definite distance, this is the reason why we have not considered the interaction time. Experimentally, time-bin encoding has been widely researched and demonstrated. Brendel *et al.* have demonstrated the time-bin encoding with time difference $(L_1-L_0)/c$ in ns orders of magnitude.[42,43] Recently, Wang *et al.* have realized the high-speed tomography of time-bin-entangled photons with the time difference 21.3 ns[44] and Takeda *et al.* have demonstrated it in a time difference 242 ns.[45] Besides, time-bin encoding has been verified as interacting with semiconductor quantum wells,[46] quantum dots,[47–49] collective atomic excitation in a rare-earth-doped solid,[50] and it has been realized in other QIP tasks.[45,51] Furthermore, Humphreys *et al.* have recently demonstrated a robust heralded controlled-phase gate with higher fidelity by using single-spatial time-bin encoding.[52] Donohue *et al.* have recently reported an effective technique using a nonlinear interaction between chirped entangled time-bin photons and shaped laser pulses to perform projective measurements on arbitrary time-bin states with ps-scale separations to readout the information of time-bin encoding.[53] That is, recent advances in Refs. [52] and Ref. [53] have provided powerful supporting for time-bin-encoding-based QIP tasks.

On the other hand, many efforts have been paid to investigate the performance of the NV centers and the coupled resonators. Although the ideal coupling strength between the NV center and optical resonator is supposed to be on the order of hundreds of megahertz, it is inevitably diminished due to some out-out-control effects.[75] Research on composite microcavity systems where NV centers in bulk diamond couple evanescently to optical resonators[65–67] makes it possible to retain the excellent properties of NV centers. The experiment in Ref. [66] provided the datum $(g,\kappa,\gamma)/2\pi\approx(0.3,26,0.0004)$ with a relative low-Q value 10^4. This datum is very close to the requirement of our proposal $g\geqslant 5\sqrt{\kappa\gamma}$, which is the same

as Ref. [61]. It deserves special mention that the NV centers used here can be replaced by any system which can realize a controlled phase flip gate.

The efficiency of our proposals is defined as the probability of the photons to be detected after the generation process. Thus, similar to the scheme proposed in Ref. [76], we use $\eta = ((r^2(\omega_{\rm in}) + r_0^2(\omega_{\rm in})/2)^n$ to denote the efficiency for GHZ state and W state, in which n denotes number of NV centers. The fidelity of the present proposal is defined as $F = |\langle\psi_{\rm ideal}|\psi_{\rm prac}\rangle|^2$, where $|\psi_{\rm ideal}\rangle$ is the ideal final state of the quantum system after processing for state generation, and $|\psi_{\rm prac}\rangle$ is the final state of the system by considering practical external reservoirs. In Fig. 9, we plot the efficiency of n-qubit state generation and fidelity of 4-qubit state generation, from which we can see that the fidelity would be higher than 92% if the condition $g^2/\kappa\gamma > 15$ is satisfied. However, it should be noted that the fidelity would decrease as the number of NV centers grow. The efficiency would be higher than 90% if the cavity parameters $g^2/\kappa\gamma$ are greater than 50 and the number of NV centers is less than 10. Nevertheless, in practical experiments, the efficiency would also be influenced by other factors; such as, the photon loss induced by the fiber and the insensitivity of the photon detector.

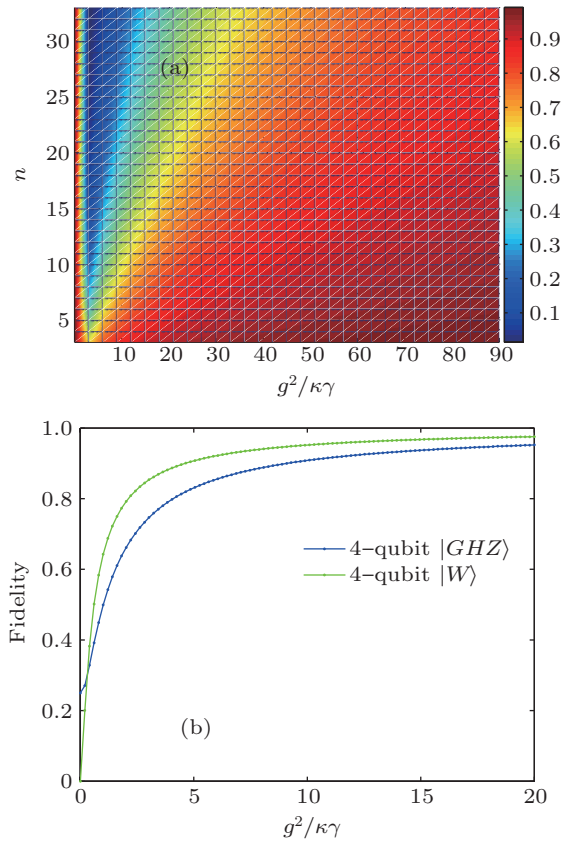


Fig. 9. (color online) (a) Efficiency of n-qubit GHZ and W-states generation. (b) Fidelity of 4-qubit GHZ and W states generation.

In conclusion, we have designed theoretical proposals to generate GHZ and W states of NV centers coupled to microresonator through noisy channels with the help of time-bin encoding processes and optical switches. The polarization and phase noise induced by noisy channels generally affect the time of state generation but not its success probability and fidelity, which is a big progress compared with the success probability 1/2 in Ref. [41]. The proposals can also be generalized to n-qubit between two nodes or among n nodes with $n-1$ different noisy channels. In addition, this proposal is robust for the regular changeable noise. For the n-qubit state generation, we here only consider the two extreme cases, i.e. two-node case and n-node case. In fact, the n-qubit state can also be generated in more than two and less than n nodes if the operators place more than one NV center in any node. In other words, our proposals provide an alternative avenue for remote large scale QIP through noisy channels via time-bin encoding.

References

[1] Ekert A K 1991 *Phys. Rev. Lett.* **67** 661
[2] Bennett C H and Wiesner S J 1992 *Phys. Rev. Lett.* **69** 2881
[3] Bennett C H, Brassard G, Crépeau C, Jozsa R, Peres A and Wootters W K 1993 *Phys. Rev. Lett.* **70** 1895
[4] Bennett C H and DiVincenzo D P 2000 *Nature* **404** 247
[5] Zhu A D, Xia Y, Fan Q B and Zhang S 2006 *Phys. Rev. A* **73** 022338
[6] Deng F G and Long G L 2004 *Phys. Rev. A* **70** 012311
[7] Karlsson A and Bourennane M 1998 *Phys. Rev. A* **58** 4394
[8] Shi B S and Tomita A 2002 *Phys. Lett. A* **296** 161
[9] Cleve R, Gottesman D and Lo H K 1999 *Phys. Rev. Lett.* **83** 648
[10] Durkin G A, Simon C and Bouwmeester D 2002 *Phys. Rev. Lett.* **88** 187902
[11] Gorbachev V N, Trubilko A I, Rodichkina A A and Zhiliba A I 2003 *Phys. Lett. A* **314** 267
[12] Gisin N and Massar S 1997 *Phys. Rev. Lett.* **79** 2153
[13] Zou X B, Pahlke K and Mathis W 2004 *Phys. Rev. A* **69** 052314
[14] Fidio C D and Vogel W 2003 *J. Opt. B: Quantum Semiclass. Opt.* **5** 105
[15] Duan L M and Kimble H J 2003 *Phys. Rev. Lett.* **90** 253601
[16] Yamamoto T, Tamaki K, Koashi M and Imoto N 2002 *Phys. Rev. A* **66** 064301
[17] Yu C S, Yi X X, Song H S and Mei D 2007 *Phys. Rev. A* **75** 044301
[18] Zheng A S, Li J H, Yu R, Lü X Y and Wu Y 2012 *Opt. Express* **20** 16902
[19] Cheng L Y, Wang H F, Zhang S and Yeon K H 2013 *Opt. Express* **21** 5988
[20] Eibl M, Kiesel N, Bourennane M, Kurtsiefer C and Weinfurter H 2004 *Phys. Rev. Lett.* **92** 077901
[21] Leibfried D, Knill E, Seidelin S, Britton J, Blakestad R B, Chiaverini J, Hume D B, Itano W M, Jost J D, Langer C, Ozeri R, Reichle R and Wineland D J 2005 *Nature* **438** 639
[22] Häffner H, Hänsel W, Roos C F, Benhelm J, Chekalkar D, Chwalla M, Körber T, Rapol U D, Riebe M, Schmidt P O, Becher C, Gühne O, Dür W and Blatt R 2005 *Nature* **438** 643
[23] Rauschenbeutel A, Nogues G, Osnaghi S, Bertet P, Brune M, Raimond J M and Haroche S 2000 *Science* **288** 2024
[24] Cirac J I, Zoller P, Kimble H J and Mabuchi H 1997 *Phys. Rev. Lett.* **78** 3221
[25] Browne D E, Plenio M B and Huelga S F 2003 *Phys. Rev. Lett.* **91** 067901
[26] Stace T M, Milburn G J and Barnes C H W 2003 *Phys. Rev. B* **67** 085317
[27] Serafini A, Mancini S and Bose S 2006 *Phys. Rev. Lett.* **96** 010503
[28] Deng Z J, Zhang X L, Wei H, Gao K L and Feng M 2007 *Phys. Rev. A* **76** 044305
[29] Li X H, Deng F G and Zhou H Y 2007 *Appl. Phys. Lett.* **91** 144101
[30] Yamamoto T, Shimamura J, Oždemir Ş K, Koashi M and Imoto N 2005 *Phys. Rev. Lett.* **95** 040503
[31] Bennett C H, Brassard G, Popescu S, Schumacher B, Smolin J A and Wootters W K 1996 *Phys. Rev. Lett.* **76** 722

[32] Sheng Y B, Zhou L, Cheng W W, Gong L Y, Zhao S M and Zheng B Y 2012 *Chin. Phys. B* **21** 030307
[33] Zheng S B 2008 *Chin. Phys. B* **17** 2969
[34] Xue P 2011 *Chin. Phys. B* **20** 100310
[35] Steane A M 1996 *Phys. Rev. Lett.* **77** 793
[36] Zhao F 2013 *Acta Phys. Sin.* **62** 200303 (in Chinese)
[37] Xiao F Y and Chen H W 2011 *Acta Phys. Sin.* **60** 080303 (in Chinese)
[38] Zhang Z R, Liu W T and Li C Z 2011 *Chin. Phys. B* **20** 050309
[39] Briegel H J, Dür W, Cirac J I and Zoller P 1998 *Phys. Rev. Lett.* **81** 5932
[40] Xue L, Nie M and Liu X H 2013 *Acta Phys. Sin.* **62** 170305 (in Chinese)
[41] Song J, Xia Y and Song H S 2008 *Phys. Rev. A* **78** 024302
[42] Brendel J, Mohler E and Martienssen W 1991 *Phys. Rev. Lett.* **66** 1142
[43] Brendel J, Gisin N, Tittel W and Zbinden H 1999 *Phys. Rev. Lett.* **82** 2594
[44] Wang S X, Chan C, Moraw P, Reilly D R, Altepeter J B and Kanter G S 2012 *Phys. Rev. A* **86** 042122
[45] Takeda S, Mizuta T, Fuwa M, Yoshikawa J I, Yonezawa H and Furusawa A 2013 *Phys. Rev. A* **87** 043803
[46] Heberle A P, Baumberg J J, Binder E, Kuhn T, Kohler K and Ploog K H 1996 *IEEE J. Sel. Top. Quantum Electron.* **2** 769
[47] Marie X, Le Jeune P, Amand T, Brousseau M, Barrau J, Paillard M and Planel R 1997 *Phys. Rev. Lett.* **79** 3222
[48] Bonadeo N H, Erland J, Gammon D, Park D, Katzer D S and Steel D G 1998 *Science* **282** 1473
[49] Michaelis de Vasconcellos S, Gordon S, Bichler M, Meier T and Zrenner A 2010 *Nat. Photon.* **4** 545
[50] Riedmatten H D, Afzelius M, Staudt M U, Simon C and Gisin N 2008 *Nature* **456** 773
[51] Takeda S, Mizuta T, Fuwa M, Loock P V and Furusawa A 2013 *Nature* **500** 315
[52] Humphreys P C, Metcalf B J, Spring J B, Moore M, Jin X M, Barbieri M, Kolthammer W S and Walmsley I A 2013 *Phys. Rev. Lett.* **111** 150501
[53] Donohue J M, Agnew M, Lavoie J and Resch K J 2013 *Phys. Rev. Lett.* **111** 153602
[54] Huang W, Wen Q Y, Jia H Y, Qin S J and Gao F 2012 *Chin. Phys. B* **21** 100308
[55] Wu G T, Zhou N R, Gong L H and Liu S Q 2014 *Acta Phys. Sin.* **63** 060302 (in Chinese)
[56] Neumann P, Mizuochi N, Rempp F, Hemmer P, Watanabe H, Yamasaki S, Jacques V, Gaebel T, Jelezko F and Wrachtrup J 2008 *Science* **320** 1326
[57] Childress L, Gurudev Dutt M V, Taylor J M, Zibrov A S, Jelezko F, Wrachtrup J, Hemmer P R and Lukin M D 2006 *Science* **314** 281
[58] Xu Z Y, Hu Y M, Yang W L, Feng M and Du J F 2009 *Phys. Rev. A* **80** 022335
[59] Dayan B, Parkins A S, Aoki T, Ostby E P, Vahala K J and Kimble H J 2008 *Science* **319** 1062
[60] Cao C, Liu G, Zhang R and Wang C 2014 *Chin. Phys. B* **23** 040304
[61] Chen Q, Yang W L, Feng M and Du J F 2011 *Phys. Rev. A* **83** 054305
[62] Lim Y L, Beige A and Kwek L C 2005 *Phys. Rev. Lett.* **95** 030505
[63] Yang W L, Yin Z Q, Xu Z Y, Feng M and Du J F 2010 *Appl. Phys. Lett.* **96** 241113
[64] Park Y S, Cook A K and Wang H L 2006 *Nano Lett.* **6** 2075
[65] Barbour R J, Dinyari K N and Wang H L 2010 *Opt. Express* **18** 18968
[66] Barclay P E, Fu K M C, Santori C and Beausoleil R G 2009 *Appl. Phys. Lett.* **95** 191115
[67] McCutcheon M W and Loncar M 2008 *Opt. Express* **16** 19136
[68] Young A, Hu C Y, Marseglia L, Harrison J P, O'Brien J L and Rarity J G 2009 *New J. Phys.* **11** 013007
[69] Buckley B B, Fuchs G D, Bassett L C and Awschalom D D 2010 *Science* **330** 1212
[70] Togan E, Chu Y, Trifonov A S, Jiang L, Maze J, Childress L, Dutt M V G, Sørensen A S, Hemmer P R, Zibrov A S and Lukin M D 2010 *Nature* **466** 730
[71] An J H, Feng M and Oh C H 2009 *Phys. Rev. A* **79** 032303
[72] Hu C Y, Young A, OBrien J L, Munro W J and Rarity J G 2008 *Phys. Rev. B* **78** 085307
[73] Su S L, Guo Q, Zhu L, Wang H F and Zhang S 2012 *J. Opt. Soc. Am. B* **29** 2827
[74] Pavičić M 2011 *Phys. Rev. Lett.* **107** 080403
[75] Barclay P E, Santori C, Fu K M, Beausoleil R G and Painter O 2009 *Opt. Express* **17** 8081
[76] Ren B C and Deng F G 2014 *Sci. Rep.* **4** 4623